Published in final edited form as:
Dev Biol. 2010 February 15; 338(2): 270–279. doi:10.1016/j.ydbio.2009.12.008.

Disruption of Paneth and goblet cell homeostasis and increased endoplasmic reticulum stress in *Agr2−/−* mice

Fang Zhao[a,d], **Robert Edwards**[b], **Diana Dizon**[a], **Jennifer R. Mastroianni**[b,e], **Mikhail Geyfman**[a], **André J. Ouellette**[b,c,e], **Bogi Andersen**[a], and **Steven M Lipkin**[a,d,*]

[a]Departments of Medicine and Biological Chemistry, University of California, Irvine

[b]Department of Pathology & Laboratory Medicine, University of California, Irvine

[c]Department of Microbiology & Molecular Genetics, School of Medicine, University of California, Irvine

Abstract

Anterior Gradient 2 (*AGR2*) is a protein disulfide isomerase that plays important roles in diverse processes in multiple cell lineages as a developmental regulator, survival factor and susceptibility gene for inflammatory bowel disease. Here, we show using germline and inducible *Agr2−/−* mice that *Agr2* plays important roles in intestinal homeostasis. *Agr2−/−* intestine has decreased goblet cell Mucin 2, dramatic expansion of the Paneth cell compartment, abnormal Paneth cell localization, elevated endoplasmic reticulum (ER) stress, severe terminal ileitis and colitis. Cell culture experiments show that *Agr2* expression is induced by ER stress, and that siRNA knockdown of *Agr2* increases ER stress response. These studies implicate *Agr2* in intestinal homeostasis and ER stress and suggest a role in the etiology of inflammatory bowel disease.

Keywords

AGR2, anterior gradient 2; intestine; Goblet cell; Paneth cell; ER stress; PDI, protein disulfide isomerase

Introduction

Anterior Gradient 2 (*AGR2*) is a developmental regulator and survival factor with multiple functions that, although highly conserved in evolution, remain poorly characterized. Originally characterized in *Xenopus* laevis, heterologous *AGR2* expression induces ectopic cement gland differentiation and alters neuronal cell fate (Aberger et al., 1998). In multiple mammalian cells,

[*]***Correspondence.*** Steven M Lipkin, Division of Gastroenterology/Hepatology, Weill Cornell Medical College, 718 Caspary, New York, NY 10021, stl2012@med.cornell.edu, Tel: 212-774-7160, Fax: 212-774-7167.
[d]Present address: Division of Gastroenterology/Hepatology, Department of Medicine, Weill Cornell Medical College, New York
[e]Present address: Department of Pathology & Laboratory Medicine, Keck School of Medicine of the University of Southern California, Los Angeles

Fang Zhao, Steven Lipkin, Bogi Andersen and Andre Ouellette participated in the study concept and design and data analysis. Fang Zhao, Diana Dizon, Jennifer Mastroianni and Mikhail Geyfman participated in data acquisition. Robert Edwards reviewed pathology.

There are no conflicts of interest to disclose for any author.

AGR2 stimulates cell proliferation, cell adhesion, motility and inhibits apoptosis (Fritzsche et al., 2006; Innes et al., 2006; Wang et al., 2008; Zhang et al., 2007). *AGR2* mRNA and protein occur at high levels in several metastatic adenocarcinomas, e.g., colorectal, esophagus, prostate, and breast, where it stimulates proliferation and inhibits apoptosis (Fritzsche et al., 2007; Fritzsche et al., 2006; Innes et al., 2006; Smirnov et al., 2005; Valladares-Ayerbes et al., 2008; Wang et al., 2008; Zhang et al., 2007). In contrast, human *AGR2* genetic variants that decrease its expression are associated with increased risk of both Crohn's disease and ulcerative colitis (Zheng et al., 2006).

Structurally, *AGR2* is a member of the endoplasmic reticulum (ER) protein disulfide isomerase (PDI) gene family (Park et al., 2009; Persson et al., 2005). PDIs facilitate the isomerization of specific client proteins into their bioactive conformations as they traffic through the ER for secretion or membrane association. When PDI substrates fail to isomerize, misfolded membrane-associated and secreted proteins accumulate in the ER, initiating ER stress, cell cycle arrest and apoptosis. For example, *AGR2* binds directly to Mucin 2 (Muc2), a major component of intestinal mucus enabling the large number of Muc2 Cys residues to pair correctly. Germline deletion of mouse *Agr2* disrupts Muc2 protein stability and decreases intestinal mucus production. However, *Agr2* deficiency is reported only to cause modest ER stress in the intestine and the impact of *Agr2* deficiency on the biology and functional state of additional intestinal cell lineages is poorly characterized (Park et al., 2009).

The lower gastrointestinal tract consists of the small intestine and colon. The lining epithelium of both organs is organized into crypts. Undifferentiated stem and progenitor cells populate the base of small intestine crypts and give rise to four major cell types: absorptive enterocytes, goblet cells, Paneth cells and enteroendocrine cells (Cheng and Leblond, 1974). Enterocytes absorb nutrients, secrete hydrolytic enzymes into the intestinal lumen and are the most common intestinal cell type. Goblet cells produce mucous to protect the intestinal barrier from infiltration by luminal contents. Paneth cells protect against microbial infection and are located at the crypt bottom. Enteroendocrine cells secrete a variety of hormones and are relatively rare. Colonic crypts contain three major cell types, including a higher proportion of goblet cells, somewhat fewer absorptive cells, and scattered enteroendocrine cells.

In normal intestine, *AGR2* is expressed in several cell types. These include mature goblet, Paneth and enteroendocrine cells, as well as Musashi-1 (MSI1)-positive intestinal stem/early progenitor cells and proliferating secretory progenitors (Wang et al., 2008).

Intestinal epithelial cells are sensitive to ER stress. Targeted deletion in the mouse of the ER stress response transcription factor XBP1s, the intestine-specific ER stress response sensor IRE1β, or mice carrying missense mutations that impair Muc2 oligomerisation and protein stability of Muc2, cause intestinal cell ER stress, cell cycle arrest, apoptosis and chronic inflammation (Bertolotti et al., 2001; Heazlewood et al., 2008; Kaser et al., 2008). Therefore, based on its structure and expression pattern, it was anticipated that *AGR2* might play a role in the intestinal ER stress response and suppression of inflammation.

Here, we show using germline and inducible *Agr2* knockout mice and siRNA knock down in cell culture that *Agr2* plays important roles in intestinal goblet and Paneth cell homeostasis, Paneth cell positioning and intestinal ER stress response. These data expand the known roles played by *Agr2* in homeostasis of the intestine.

Materials and methods

Generation of Agr2−/− mice

The gene-targeting strategy is described in supplementary methods and summarized in Fig. 1. Mice were housed in a temperature (~21°C) and humid ity (~55%)-controlled room in an AALAC accredited vivarium with a 12 h light :12 h dark cycle. Entry into the vivarium was restricted to appropriate personnel, but no SPF precautions were available. Food pellets (Research Diets, New Jersey) and water were available ad libitum.

Histology, immunohistochemistry and immunofluorescence

Mouse intestines were removed and washed in cold phosphate-buffered saline (PBS), fixed by immersion in 4% paraformaldehyde, embedded in paraffin, and 5 μm sections were applied to Probe-on Plus™ slides (Fisher). For histology review, sections were stained with Hematoxylin and Eosin or Alcian blue and nuclear fast red as detailed in supplementary methods For immunohistochemistry, primary antibodies and according biotinylated secondary antibodies were using. Staining was detected with Vectastain ABC reagent (PK-6100, Vector) and development with DAB chromogen (DakoCytomation). For immunofluorescence, primary antibodies and according Texas red or fluorescein labeled secondary antibody were applied, then slides were covered with Vectashield mounting medium with DAPI (H-1200, Vector). For details and sources of antibodies, please refer to supplementary methods.

BrdU labeling proliferation assay

To test proliferation, mice were injected 2 hours before sacrifice with BrdU labeling reagent. Tissues were processed and the BrdU labeling cell proliferation assay were performed according to the manufacturer's protocol (BrdU labeling and Detection Kit I, Roche).

Epithelial RNA isolation and quantification

Sheets of small intestinal epithelium were separated from underlying lamina propria using 3 mM EDTA, 0.5 mM DTT in PBS (Whitehead et al., 1993). Briefly, mouse intestine was removed, opened and washed in PBS 3 changes. The linearized intestine was decontaminated by soaking in 0.04% (vol/vol) sodium hypochlorite in PBS for 20 minutes at room temperature, then incubated in 3mM EDTA plus 0.5mM DTT in PBS at 22°C for 90 minutes with occasional gentle stirring. The digestion mixture of the intestine was resuspended in PBS and epithelium detached by vigorous shaking in a sealed container. Intestinal epithelium was harvested by centrifuge at 1000rpm for 5minutes. Total RNA isolated using Qiagen RNAeasy columns was reverse transcribed to cDNA by using cDNA Kit (Applied Biosystems). qRT-PCR was performed using an ABI 7900HT-SequenceDetection System with SYBR Green Master Mix. For quantitative analysis, all samples were normalized to *Gapdh* expression using the ΔΔCT value method. Gene-specific primers refer to supplementary methods.

Western blot

Samples were separated by SDS/PAGE and transferred to Immobilon-P PVDF (Millipore). Membranes were blocked with 5% nonfat dry milk and incubated overnight at 4 °C with primary antibodies. Band was detected by chemiluminesence using HRP-conjugated secondary antibody and ECL Western blotting reagents (GE Healthcare).

Purification and analysis of Cryptdin peptides

Cryptdin peptides were isolated using modified procedures described previously (Mastroianni and Ouellette, 2009; Selsted et al., 1992). Ilea were excised from seven inducible *Agr2*−/− mice (after 4 days of tamoxifen administration) and seven wild type mice (also received tamoxifen

administration for 4 days). Protein extracts were prepared from "complete" ileum, consisting of tissue plus luminal contents. Details refer to supplementary methods.

XBP1 splicing assay

XBP1 splicing was measured by specific primers (Kaser et al., 2008) flanking the splicing site yielding PCR product sizes of 164 and 138 bp for human *XBP1u* and *XBP1s*, and 171 and 145 bp for mouse *Xbp1*. Products were resolved on 2% agarose gels and band intensity was determined densitometrically.

Cell line and small interfering RNA (siRNA) transient transfections

Pancreatic cancer cell line, Su.86.86 (American Type Culture Collection) and ON-TARGETplus SMARTpool Human siRNA-*AGR2* and Non-targeting Pool control scrambled siRNA (siRNA-Scr) (Dharmacon, Inc.) were used. Details are described in supplementary methods.

SuperArray Screening

Epithelial RNA was converted to cDNA using RT^2 first strand kit (SABioscience, C-03). Real-time PCR was done using SuperArray RT^2 SYBR Green qPCR Master Mix (SABioscience, PA-012-12) and SuperArray RT^2 Profiler™ PCR Array (PAMM−077). Thermal cycling parameters were 95°C for 10 min, followed by 40 cycles of amplifications at 95°C for 15s, 60° C for 60s. Data was analyzed by PCR Array Data Analysis Web Portal using the default set format.

In situ hybridization

Mouse ileum was fixed in 4% paraformaldehyde at 4°C overnight, then transferred to 30% sucrose solution and incubated at 4°C overnight, finally fr ozen in OCT compound and stored at −80°C. In situ hybridization was performed with 10-μm cryosections as described (Abzhanov et al., 2003). Details refer to supplementary methods.

Results

Generation of germline and inducible Agr2 −/− Mice

To understand the mechanistic roles of *Agr2* we created a *Cre-LoxP* inducible *Agr2* knockout mouse model (Fig. 1**A**). To generate a germline *Agr2−/−* mice we crossed *Protamine-Cre* transgenic mice (O'Gorman et al., 1997) (*Tg PRM-Cre*) that deletes *Agr2* in the male germline. For detailed breeding strategies, see Fig. 1**B**. We then intercrossed *Agr2 flox/−* mice to make *Agr2−/−* mice. To generate inducible *Agr2−/−* mice, we used the *Rosa26-CreER* strain that has tightly controlled and inducible systemic *Cre* recombinase activation with tamoxifen (Badea et al., 2003). We crossed the *Rosa26-CreER* (*Tg Tam-Cre*) with *Agr2 flox/flox* to create *Agr2flox/flox;TgTam-Cre* mice to create inducible *Agr2−/−* mice. *Agr2flox/flox;TgTam-Cre* mice express *Agr2* until mice are injected with tamoxifen (Garcia and Mills, 2002). For both germline and inducible *Agr2−/−* mice, deletions of exons 2,3 and 4 were confirmed by sequencing of cDNA converting from RNA isolated from intestine epithelia (Fig. 1**D**). *Agr2* protein was undetectable as assayed by western blotting and IHC (Fig. 1**E,F**). Our models are therefore a null allele.

Dramatically decreased Mucin 2 in goblet cells from germline and inducible Agr2−/− mice

To analyze the phenotype in GI tract of *Agr2−/−* mice, we performed H+E staining which showed that germline and inducible *Agr2−/−* mice lack morphologically normal goblet cells (Supplementary Fig. 1**A,B,C**). Next, we performed Alcian Blue staining. Alcian Blue detects acid mucopolysaccharides and glycosaminoglycans, which are normally restricted to pre-

goblet and goblet cells. Staining of wild type small intestine revealed numerous Alcian Blue-positive cells (Supplementary Fig. 1**D**). By contrast, virtually no Alcian Blue-positive cells were observed in either germline or inducible *Agr2−/−* mice(Supplementary Fig. 1**E,F**). Immunohistochemistry revealed that MUC2 protein was dramatically reduced, but detectable (Supplementary Fig. 1**G,H,I**). In contrast, the goblet cell marker intestinal trefoil factor (ITF) was not reduced in germline *Agr2−/−* mice (Supplementary Fig.1**J,K**). No significant differences in intestinal enteroendocrine cell chromogranin A were seen (Supplementary Fig. 1**S,T,U**). In summary, the goblet cell lineage continues to exist in both germline and inducible *Agr2−/−* small intestine but these cells lose their normal morphology and cannot be identified by H&E or Alcian blue staining.

Multiple Paneth cell abnormalities in Agr2−/− mice

Paneth cells are specialized epithelial cells that mediate innate mucosal immunity against enteric microbial infections. Localized at the base of the crypts of Lieberkühn in the small intestine, Paneth cells release large, apically-oriented dense-core secretory granules containing cryptdins and other host defense molecules (Porter et al., 2002). Dramatic expansion of Paneth cell compartment was consistently seen in all regions of the small intestine both in the germline and inducible *Agr2−/−* mice (Fig. 2**A**) (Supplementary Fig. 2). These cells containing large, dense eosinophilic granules were confirmed to be Paneth cells with immunostudies of markers cryptdin-5, MMP7, lysozyme and Sox9 (Supplementary Figs. 1,3). Cells immunopositive for these Paneth cell markers were detected in wild type small intestine and limited to the bottom of crypts. These cells comprised a visibly greater proportion of the crypt base in both germline (Supplementary Fig. 1**N,Q**) and inducible (Supplementary Fig. 1**O,R**) *Agr2−/−* intestine. To confirm these studies, we examined *Sox9* mRNA expression, which is elevated more than five-fold (Fig. 2**C**) and mature cryptdin peptides, which are elevated more than three-fold vs wild type mice (Fig. 2**D**) in inducible *Agr2−/−* intestine. Additionally, cells containing large, dense eosinophilic granules are abnormally positioned in the villi of germline *Agr2−/−* small intestine. Cells with dense large granules are also immunopositive for Paneth cell markers cryptdin-5, MMP7, lysozyme and Sox9 (Fig. 2**B** and Supplementary Fig. 3).

Terminal ileitis and colitis in Agr2−/− mice

To define in more detail the normal *Agr2* expression pattern in wild-type mice, we analyzed the entire lower GI tract by immunohistochemistry and Western blot analysis. *Agr2* is expressed in all regions of small intestine and colon. Highest expression is in the ileum and colon (Supplementary Fig. 4). In both germline and inducible *Agr2−/−* mice, in addition to Paneth cell compartment expansion and decreased Mucin 2 expression in goblet cells we see profound inflammatory infiltrates in the lamina propria and submucosa. The inflammation is most severe in the terminal ileum, and to a lesser extent in the colon. In the germline *Agr2−/−* mice, the terminal ileitis is characterized by a dense neutrophilic infiltrate surrounding both crypt bases and submucosal perivascular spaces (Fig. 3**A**, **inset**). There is marked follicular hyperplasia of the Peyer's patches, which also have numerous multinucleated giant cells in the interfollicular areas, suggestive of granulomatous inflammation (Fig. 3**C,D**, **arrows**). Germline deletion of *Agr2* in the colon causes colitis, characterized by a mixed acute and chronic inflammatory infiltrate expanding the isolated lymphoid follicles and the lamina propria. There is significant neutrophil infiltration and marked crypt hyperplasia (Fig. 3**B**). No inflammation or other abnormalities were seen in *Tam-Cre* mice without the *Agr2 flox/flox* alleles (data not shown). In summary, both germline and inducible *Agr2−/−* mice have dramatic inflammation of the intestine, most notably the ileum, and colon.

Paneth cell abnormalities precede those of goblet cells and enterocytes

Because germline *Agr2−/−* mice have a dramatic increase in both Paneth cells and inflammation, it could not be defined whether Paneth cell expansion was a primary response to acute *Agr2* deficiency or a response to inflammation and bacterial invasion from a compromised intestinal epithelial barrier. To resolve this issue, we firstly analyzed the inducible *Agr2−/−* model at multiple time points after induced deletion. After inducing *Agr2* knockout, the first observable defect is Paneth cell expansion 24 hours after tamoxifen injection (day 1) (Fig. 4**A**). Importantly, this Paneth cell abnormality precedes any histologic signs of inflammation. Subsequently, normal goblet cells are lost and acute inflammatory infiltrates invade the lamina propria, along with a further increase in the Paneth cell compartment (day 3). Next, enterocyte homeostasis is disrupted as the remaining absorptive enterocytes become dysplastic and the villi are blunted (day 5). To test further whether 24 hours after *Agr2* deletion there is an early inflammatory response that could explain the observed Paneth cell expansion, we analyzed expression of MUC2, acid mucins (with Alcian blue staining) and 82 key genes involved in mouse inflammatory responses using SuperArray profiling. Compared to wild type mice, MUC2 immunofluorescence and Alcian blue staining at this time point are not changed (Supplementary Fig. 5), and SuperArray profiling reveals only one significantly dysregulated gene (*Nos2*) 24 hours after *Agr2* deletion in small intestine epithelium (Supplementary Fig. 6). However, on day 5 after *Agr2* deletion, when there is notable inflammation, MUC2 immunofluorescence, alcian blue staining of acid mucins are dramatically decreased (Supplementary Fig. 1**I,F**) and 47 out of 82 SuperArray profiled genes are dysregulated (data not shown). To test whether the impact of *Agr2* deletion on enterocytes is caused by decreased proliferation or increased apoptosis, we performed BrdU and caspase 3 staining of wild type and induced *Agr2−/−* small intestine and colon. By day 6, the induced *Agr2* deletion caused significantly less proliferation and increased apoptosis in all regions of the small intestine and colon (Fig. 4**B,C**). In summary, the first observable defect after *Agr2* induced knockout is Paneth cell hypertrophy and expansion followed by loss of visible goblet cells, and subsequent decreased enterocyte proliferation and increased apoptosis.

Increased ER stress in Agr2 knockout intestine and siRNA knockdown cells

Based on its structure and expression pattern, it was originally anticipated that *AGR2* might play a role in the intestinal ER stress response. However, in a previous study of *Agr2−/−* mice, only modestly increased ER stress markers at the mRNA level were found (Park et al., 2009). The ER chaperone BiP and the spliced form of Xbp1 (Xbp1s) are well characterized biomarkers of ER stress (Ron and Walter, 2007). Therefore, we analyzed their expression in *Agr2−/−* intestinal epithelial preps. BiP protein levels were dramatically increased in germline *Agr2−/−* small intestine (Fig. 5**A**). To explore the expression pattern of BiP in small intestine, we first performed in situ hybridization by using a digoxigenin-labeled antisense RNA probe and a sense control probe specific for BiP. In wild type mice, the hybridization signal was detected in epithelial cells of the middle and upper crypts and at crypt-villus junctions (Supplementary Fig. 7**A**). In germline *Agr2−/−* mice, increased signal intensity was evident in the same regions as wild type mice but also extending into the lower regions of crypts and villi (Supplementary Fig. 7**B**). Additionally, certain epithelial cells with increased BiP hybridization signals were seen in the upper villus regions (Supplementary Fig. 7**B**, **black arrows**) as well as in cells adjacent to Paneth cells near and at the base of crypts (Supplementary Fig. 7**F**). No detectable signals were detected at the upper villi or crypt base of wild type mice (Supplementary Fig. 7**E**). As *Agr2* is normally expressed in multiple cell types including all three mature secretory cell lineages and MSI1-positive intestinal stem cells/early progenitor cells (Wang et al., 2008), we performed co-immunofluorescence studies to understand which cell types experience ER stress. BiP protein is increased is MSI1-positive cells at the crypt base (Supplementary Fig. 8**A**, white arrow) and lower crypt proliferative zone (Supplementary Fig. 8**B**, **white arrows**). Additionally, both ITF-positive goblet cells and abnormally positioned

MMP7-positive Paneth cells on villi have increased BiP protein (Supplementary Fig. 8**C,D**). In summary, protein levels of the ER stress marker BiP are increased in MSI1-positive intestinal stem/early progenitor cells as well as in cells on villi that are immunopositive for goblet cell and Paneth cell lineage markers.

To examine ER stress in more detail, we analyzed other markers. In wild type mice, Xbp1u mRNA was detectable but Xbp1s mRNA level was not. In contrast, Xbp1s mRNA was expressed in *Agr2−/−* mice (Fig. 5**B**). mRNA levels for additional ER stress response markers *Chop, Pdia3* and *Perk* also were elevated (Fig. 5**C**).

Because the intestine has a complex physiology and is populated with many different cell types, we could not determine whether the impact of *Agr2* deletion directly or indirectly increases intestinal ER stress. To confirm the observations in *Agr2−/−* intestine and test whether *Agr2* plays a direct role in this process, we used a different experimental approach, siRNA knockdown studies in cell culture. First, we tested whether *AGR2* is an ER stress response gene. In SU86.86 cells, baseline *AGR2* protein levels are low. Tunicamycin is a well characterized inhibitor of ER protein glycosylation and inducer of ER stress. Treatment with tunicamycin significantly increases *AGR2* protein levels (Fig. 6**A**). Next, we looked at protein levels of the ER chaperone and ER stress response gene BiP. In untreated cells transfected with control scrambled siRNA, protein levels of the ER stress biomarker BiP are low (Fig. 6**B**). siRNA knockdown of *AGR2* in cells effectively decreases *AGR2* protein levels, but does not affect basal BiP levels. As expected, treatment with the ER stress inducer tunicamycin increases BiP levels. siRNA knockdown of *AGR2* in tunicamycin treated cells further increases BiP protein levels. Consistent with Fig. 6**A**, *AGR2* protein levels are also induced by tunicamycin, while control β-actin levels are not. Next, we tested for XBP1s. As expected, tunicamycin increases the ratio of spliced (active in ER stress) to unspliced XBP1 (XBP1s/u). siRNA knockdown in untreated cells only slightly increased the XBP1s/u ratio. However, in the presence of tunicamycin, siRNA knockdown of *Agr2* significantly increased the XBP1s/u ratio (Fig. 6**C,D**).

Discussion

AGR2 is an evolutionarily highly conserved protein disulfide isomerase whose roles include stimulation of cell proliferation, adhesion, motility, anti-apoptosis, Muc2 protein folding and developmental cell fate (Aberger et al., 1998; Fritzsche et al., 2007; Fritzsche et al., 2006; Innes et al., 2006; Smirnov et al., 2005; Valladares-Ayerbes et al., 2008; Wang et al., 2008; Zhang et al., 2007). In the intestine, *AGR2* is strongly expressed in several distinct cell types, including the three differentiated intestinal secretory cell lineages, goblet cell progenitors and MSI1-positive intestinal stem cells/early progenitors (Wang et al., 2008). Because of this expression pattern and the fact that each protein disulfide isomerase is thought to have multiple client substrates, it was originally anticipated that *AGR2* would play diverse roles in multiple intestinal cell types. Our experiments indicate that the absence of *Agr2* can lead to abnormalities in multiple intestinal cell types and increased ER stress.

A recent study using germline *Agr2−/−* mice showed that this gene plays an essential role in the production of intestinal mucus by goblet cells(Park et al., 2009). However, in the absence of exogenous agents, there were no other abnormalities in intestinal physiology, homeostasis, or inflammation of the small intestine or colon noted. In our study, we generated germline and inducible *Agr2−/−* mouse models. Consistent with this study (Park et al., 2009), our germline and inducible *Agr2−/−* mice have virtually no morphologically normal goblet cells and decreased intestinal mucus. Also consistent with this study, the goblet cell lineage still exists and there is no apparent enteroendocrine cell phenotype.

However, in contrast to the previous study, we observe several additional abnormalities. These include dramatic intestinal Paneth cell abnormalities and severe intestinal inflammation in the absence of treatment with any exogenous agents. The Paneth cell expansion occurs along the whole small intestine and is most dramatic in the ileum. Extracellular Paneth cell granule aggregations and even casts commonly occur. Consistent with expansion of the Paneth cell compartment, expression of differentiated Paneth cell markers *Sox9* and cryptdin-5 are dramatically elevated.

Another abnormality in the germline *Agr2*−/− mice is mislocalized Paneth cells away from the crypt base into the upper crypt and villi. This abnormal Paneth cell location phenotype is also seen in mouse knockouts of the *WNT* signaling components *Frizzled 5*, *EphB3* and *Apc* that help specify proper cell location along the crypt-villus axis (Andreu et al., 2008; Batlle et al., 2002; van Es et al., 2005). Because *Sox9* is a feedback inhibitor of *WNT* signaling, it is possible that the increased *Sox9* expression in *Agr2*−/− intestine inhibits *Frizzled 5*, *EphB3* or *Apc* expression and/or activity to cause inappropriate Paneth cell migration. Future studies with inducible *Sox9* transgenic mice may help to answer this question.

Because Paneth cells can respond to inflammation, we performed a time course with inducible *Agr2*−/− mice to determine if inflammation preceded the Paneth cell increase or the reverse sequence was occurring. Expansion of the Paneth cell compartment is the first morphological abnormality caused by induced *Agr2* deficiency and precedes any signs of intestinal inflammation or decreased intestinal mucus production. In summary, while we cannot exclude a low level inflammatory response 24 hours after *Agr2* induced deletion that we did not detect is responsible for the expansion of the Paneth cell compartment, our data are most consistent with Paneth cell abnormalities being the first observable change from induced *Agr2* deletion, followed by loss of normal goblet cells and mucin secretion. Future studies will be required to address whether expansion of the Paneth cell compartment truly is a primary effect of induced *Agr2* deletion, or if inflammation below the detection level of our studies is causing this expansion. Because a recent study observed the morphological loss of goblet cells without any Paneth cell abnormalities, the mechanism of *Agr2* action to inhibit goblet cell mucus production and impair normal morphology is likely to be distinct from that causing Paneth cell expansion. This interpretation is also consistent with previous observations that transgenic ablation of goblet cells does not cause spontaneous inflammation or Paneth cell expansion (Itoh et al., 1999), both of which are seen in *Agr2*−/− mice. Finally, in the inducible *Agr2*−/− model, subsequent to Paneth and goblet cell abnormalities and inflammation, enterocyte homeostasis is disrupted with decreased proliferation, increased apoptosis and blunting of villi. Because *Sox9* knockout in intestinal epithelium causes increased enterocyte proliferation, hyperplasia and Paneth cell loss (the opposite of the *Agr2*−/− phenotype), it is possible these effects are mediated through increased levels of *Sox9* in inducible *Agr2*−/− mice. However, given the delay in enterocyte abnormalities, these effects may well be secondary to problems occurring in other cell types rather than a primary effect of *Agr2* deficiency. Future studies with intestinal cell type specific *Agr2* deletion will be helpful to resolve this issue.

We do not see abnormally positioned Paneth cell in the inducible *Agr2*−/− mice, nor do not see decreased proliferation or increased apoptosis of enterocytes in the germline *Agr2*−/− mice. The reasons for these differences are not clear at present. With regard to the Paneth cell location, the acute significant disruption of crypt-villus architecture in the inducible *Agr2*−/− mice may preclude abnormal Paneth cell migration or differentiation in the upper crypt and villus, if it were to occur. With regard to decreased proliferation and increased apoptosis of enterocytes and overall disruption of crypt-villus architecture in the inducible but not germline *Agr2*−/− mice, we speculate that this difference may reflect a gradual upregulation of other protein disulfide isomerases during development in the germline knockout mice that compensate for the loss of *Agr2*. However, with inducible *Agr2* knockout, intestinal cells cannot compensate

for the acute loss. The lack of acute compensation causes increased cellular apoptosis and decreased proliferation. Future studies to identify other protein disulfide isomerases that can compensate for *Agr2* loss may help to resolve this issue.

Our *Agr2*−/− mice develop severe acute terminal ileitis with multinucleated giant cells reminiscent of granulomatous inflammation. Overall, our findings in the germline knockouts are similar to that seen in human Crohn's disease. In molecular epidemiology studies, *AGR2* genetic variants that decrease its mRNA expression are associated with increased risk of both Crohn's disease and ulcerative colitis(Zheng et al., 2006). While there are multiple mouse models used for the study of ulcerative colitis(Byrne and Viney, 2006; Jurjus et al., 2004) to our knowledge only $TNF^{\Delta ARE}$ and SAMP1/Yit mice are currently used as models of Crohn's disease (Bamias et al., 2007). Therefore, further studies of *Agr2*−/− mice may be particularly helpful to improve our mechanistic understanding of Crohn's disease etiology.

ER stress causes cells to arrest proliferation and initiate apoptosis. Targeted deletion of the mouse ER stress response transcription factor Xbp1, the GI epithelial specific ER stress response gene Ire1β or mice carrying missense mutations in Muc2 and Mtbtps1 that increase GI epithelial cell ER stress cause decreased intestinal enterocyte proliferation, increased apoptosis, and inflammation (Bertolotti et al., 2001; Brandl et al., 2009; Heazlewood et al., 2008; Kaser et al., 2008). Protein disulfide isomerases relieve ER stress and *Agr2* was previously speculated to play a role in the ER stress response (Persson et al., 2005). In our *Agr2*−/− mice, we find elevated intestinal levels of ER stress. ER stress is high in proliferating MSI1-positive intestinal stem cell/early progenitor cells, ITF-positive goblet lineage cells and MMP7-positive abnormally positioned Paneth cells in the villus in *Agr2*−/− small intestine. Surprisingly, there is no increased ER stress in the mature Paneth cells at the crypt base. Future experiments with cell lineage specific *Agr2* knockout mice will be necessary to understand more precisely the role of *Agr2* in the different intestinal cell types, and whether these are the same cells experiencing ER stress in Xbp1, Ire1β, Muc2 and Mtbtps1 mouse models of inflammatory bowel disease. Additionally, these experiments will help address the role of cell autonomous and non-cell autonomous increased ER stress in the intestine.

To confirm whether *Agr2* deficiency increases ER stress, and test whether this effect is a direct rather than indirect consequence of *Agr2* deficiency, we performed siRNA knockdown of *Agr2* in cell culture. We found *Agr2* protein levels increase in response to ER stress and that *Agr2* knockdown causes increased ER stress levels in cells treated with the ER stress inducer tunicamycin.

In the previous study of *Agr2*−/− mice, the authors concluded that ER stress was not significantly elevated in this model. However, in their model the intestinal inflammation was not seen in the small intestine and extremely mild in the colon in the absence of treatment with the colitis inducer DSS(Park et al., 2009). It is not clear at present why in our *Agr2*−/− mouse lines intestinal inflammation is more severe, and several intestinal cell types are affected, compared to only goblet cell Muc2 production and increased DSS sensitivity in the line developed previously. In our model, we engineered deletion of *Agr2* exons 2–4, while the other group deleted exons 2–3. We also cannot exclude differences in genetic background as a potential cause. For example, the C57B/L6 strain is largely resistant to intestinal inflammation by DSS and in *Muc2*−/− mice the colitis phenotype arises only on a permissive genetic background (Velcich et al., 2002). However, perhaps a more likely explanation is that the mice generated previously were housed in a germ free barrier facility while our mice were not. Therefore, it is tempting to speculate that commensal flora in our *Agr2*−/− colony contribute to the broader expressivity and increased severity of the pathology, most notably in the development of terminal ileitis. Commensal microflora have been suggested to worsen the severity of terminal ileitis in the SAMP1/YitFc model of Crohn's disease(Bamias et al.,

2007). This speculation would be consistent with our cell culture studies as well, where *Agr2* knockdown in isolation did not much affect basal ER stress levels but had a significant effect when cells were treated exogenously with an ER stress inducing agent. Future studies that examine *Agr2*−/− intestinal inflammation in germ free conditions with exposure to individual, well characterized strains of commensal bacteria will be helpful to address this question. Since human *AGR2* genetic variants that decrease its expression are associated with increased risk of Crohn's disease and ulcerative colitis(Zheng et al., 2006), further experiments studying gene/environment interactions in *Agr2*−/− mice and cells may well provide important insights into the etiology of Crohn's disease and ulcerative colitis.

Supplementary Material

Refer to Web version on PubMed Central for supplementary material.

Acknowledgments

Grant Support: NIH Grants DK044632, AI059346 (A.J.O.); Institutional funds (S.M. L.); NIH Grants AR 44882 (B.A.).

Abbreviations

AGR2	*Anterior Gradient 2*
ER	endoplasmic reticulum
PDI	protein disulfide isomerase
BrdU	bromodeoxyuridine

References

Aberger F, Weidinger G, Grunz H, Richter K. Anterior specification of embryonic ectoderm: the role of the Xenopus cement gland-specific gene XAG-2. Mech Dev 1998;72:115–130. [PubMed: 9533957]

Abzhanov A, Tzahor E, Lassar AB, Tabin CJ. Dissimilar regulation of cell differentiation in mesencephalic (cranial) and sacral (trunk) neural crest cells in vitro. Development (Cambridge, England) 2003;130:4567–4579.

Andreu P, Peignon G, Slomianny C, Taketo MM, Colnot S, Robine S, Lamarque D, Laurent-Puig P, Perret C, Romagnolo B. A genetic study of the role of the Wnt/beta-catenin signalling in Paneth cell differentiation. Developmental biology 2008;324:288–296. [PubMed: 18948094]

Badea TC, Wang Y, Nathans J. A noninvasive genetic/pharmacologic strategy for visualizing cell morphology and clonal relationships in the mouse. J Neurosci 2003;23:2314–2322. [PubMed: 12657690]

Bamias G, Okazawa A, Rivera-Nieves J, Arseneau KO, De La Rue SA, Pizarro TT, Cominelli F. Commensal bacteria exacerbate intestinal inflammation but are not essential for the development of murine ileitis. J Immunol 2007;178:1809–1818. [PubMed: 17237431]

Barker N, Clevers H. Tracking down the stem cells of the intestine: strategies to identify adult stem cells. Gastroenterology 2007;133:1755–1760. [PubMed: 18054544]

Barker N, van de Wetering M, Clevers H. The intestinal stem cell. Genes Dev 2008;22:1856–1864. [PubMed: 18628392]

Bastide P, Darido C, Pannequin J, Kist R, Robine S, Marty-Double C, Bibeau F, Scherer G, Joubert D, Hollande F, Blache P, Jay P. Sox9 regulates cell proliferation and is required for Paneth cell differentiation in the intestinal epithelium. J Cell Biol 2007;178:635–648. [PubMed: 17698607]

Batlle E, Henderson JT, Beghtel H, van den Born MM, Sancho E, Huls G, Meeldijk J, Robertson J, van de Wetering M, Pawson T, Clevers H. Beta-catenin and TCF mediate cell positioning in the intestinal epithelium by controlling the expression of EphB/ephrinB. Cell 2002;111:251–263. [PubMed: 12408869]

Bertolotti A, Wang X, Novoa I, Jungreis R, Schlessinger K, Cho JH, West AB, Ron D. Increased sensitivity to dextran sodium sulfate colitis in IRE1beta-deficient mice. J Clin Invest 2001;107:585–593. [PubMed: 11238559]

Brandl K, Rutschmann S, Li X, Du X, Xiao N, Schnabl B, Brenner DA, Beutler B. Enhanced sensitivity to DSS colitis caused by a hypomorphic Mbtps1 mutation disrupting the ATF6-driven unfolded protein response. Proceedings of the National Academy of Sciences of the United States of America 2009;106:3300–3305. [PubMed: 19202076]

Byrne FR, Viney JL. Mouse models of inflammatory bowel disease. Current Opinion in Drug Discovery & Development 2006;9:207–217.

Cheng H, Leblond CP. Origin, differentiation and renewal of the four main epithelial cell types in the mouse small intestine. V. Unitarian Theory of the origin of the four epithelial cell types. American Journal of Anatomy 1974;141:537–561. [PubMed: 4440635]

Fritzsche FR, Dahl E, Dankof A, Burkhardt M, Pahl S, Petersen I, Dietel M, Kristiansen G. Expression of AGR2 in non small cell lung cancer. Histol Histopathol 2007;22:703–708. [PubMed: 17455144]

Fritzsche FR, Dahl E, Pahl S, Burkhardt M, Luo J, Mayordomo E, Gansukh T, Dankof A, Knuechel R, Denkert C, Winzer KJ, Dietel M, Kristiansen G. Prognostic relevance of AGR2 expression in breast cancer. Clin Cancer Res 2006;12:1728–1734. [PubMed: 16551856]

Garcia EL, Mills AA. Getting around lethality with inducible Cre-mediated excision. Semin Cell Dev Biol 2002;13:151–158. [PubMed: 12127267]

Heazlewood CK, Cook MC, Eri R, Price GR, Tauro SB, Taupin D, Thornton DJ, Png CW, Crockford TL, Cornall RJ, Adams R, Kato M, Nelms KA, Hong NA, Florin TH, Goodnow CC, McGuckin MA. Aberrant mucin assembly in mice causes endoplasmic reticulum stress and spontaneous inflammation resembling ulcerative colitis. PLoS Med 2008;5:e54. [PubMed: 18318598]

Innes HE, Liu D, Barraclough R, Davies MP, O'Neill PA, Platt-Higgins A, de Silva Rudland S, Sibson DR, Rudland PS. Significance of the metastasis-inducing protein AGR2 for outcome in hormonally treated breast cancer patients. Br J Cancer 2006;94:1057–1065. [PubMed: 16598187]

Itoh H, Beck PL, Inoue N, Xavier R, Podolsky DK. A paradoxical reduction in susceptibility to colonic injury upon targeted transgenic ablation of goblet cells. J Clin Invest 1999;104:1539–1547. [PubMed: 10587517]

Jurjus AR, Khoury NN, Reimund JM. Animal models of inflammatory bowel disease. Journal of Pharmacological & Toxicological Methods 2004;50:81–92. [PubMed: 15385082]

Kaser A, Lee AH, Franke A, Glickman JN, Zeissig S, Tilg H, Nieuwenhuis EE, Higgins DE, Schreiber S, Glimcher LH, Blumberg RS. XBP1 links ER stress to intestinal inflammation and confers genetic risk for human inflammatory bowel disease. Cell 2008;134:743–756. [PubMed: 18775308]

Mastroianni JR, Ouellette AJ. Alpha-defensins in enteric innate immunity: functional Paneth cell alpha-defensins in mouse colonic lumen. The Journal of biological chemistry 2009;284:27848–27856. [PubMed: 19687006]

Mori-Akiyama Y, van den Born M, van Es JH, Hamilton SR, Adams HP, Zhang J, Clevers H, de Crombrugghe B. SOX9 is required for the differentiation of paneth cells in the intestinal epithelium. Gastroenterology 2007;133:539–546. [PubMed: 17681175]

O'Gorman S, Dagenais NA, Qian M, Marchuk Y. Protamine-Cre recombinase transgenes efficiently recombine target sequences in the male germ line of mice, but not in embryonic stem cells. Proceedings of the National Academy of Sciences of the United States of America 1997;94:14602–14607. [PubMed: 9405659]

Park SW, Zhen G, Verhaeghe C, Nakagami Y, Nguyenvu LT, Barczak AJ, Killeen N, Erle DJ. The protein disulfide isomerase AGR2 is essential for production of intestinal mucus. Proc Natl Acad Sci U S A 2009;106:6950–6955. [PubMed: 19359471]

Persson S, Rosenquist M, Knoblach B, Khosravi-Far R, Sommarin M, Michalak M. Diversity of the protein disulfide isomerase family: identification of breast tumor induced Hag2 and Hag3 as novel members of the protein family. Mol Phylogenet Evol 2005;36:734–740. [PubMed: 15935701]

Porter EM, Bevins CL, Ghosh D, Ganz T. The multifaceted Paneth cell. Cell Mol Life Sci 2002;59:156–170. [PubMed: 11846026]

Ron D, Walter P. Signal integration in the endoplasmic reticulum unfolded protein response. Nature Reviews Molecular Cell Biology 2007;8:519–529.

Selsted ME, Miller SI, Henschen AH, Ouellette AJ. Enteric defensins: antibiotic peptide components of intestinal host defense. Journal of Cell Biology 1992;118:929–936. [PubMed: 1500431]

Smirnov DA, Zweitzig DR, Foulk BW, Miller MC, Doyle GV, Pienta KJ, Meropol NJ, Weiner LM, Cohen SJ, Moreno JG, Connelly MC, Terstappen LW, O'Hara SM. Global gene expression profiling of circulating tumor cells. Cancer Res 2005;65:4993–4997. [PubMed: 15958538]

Valladares-Ayerbes M, Diaz-Prado S, Reboredo M, Medina V, Iglesias-Diaz P, Lorenzo-Patino MJ, Campelo RG, Haz M, Santamarina I, Anton-Aparicio LM. Bioinformatics approach to mRNA markers discovery for detection of circulating tumor cells in patients with gastrointestinal cancer. Cancer Detect Prev 2008;32:236–250. [PubMed: 18801625]

van Es JH, Jay P, Gregorieff A, van Gijn ME, Jonkheer S, Hatzis P, Thiele A, van den Born M, Begthel H, Brabletz T, Taketo MM, Clevers H. Wnt signalling induces maturation of Paneth cells in intestinal crypts. Nat Cell Biol 2005;7:381–386. [PubMed: 15778706]

Velcich A, Yang W, Heyer J, Fragale A, Nicholas C, Viani S, Kucherlapati R, Lipkin M, Yang K, Augenlicht L. Colorectal cancer in mice genetically deficient in the mucin Muc2. Science 2002;295:1726–1729. [PubMed: 11872843]

Wang Z, Hao Y, Lowe AW. The adenocarcinoma-associated antigen, AGR2, promotes tumor growth, cell migration, and cellular transformation. Cancer Res 2008;68:492–497. [PubMed: 18199544]

Whitehead RH, VanEeden PE, Noble MD, Ataliotis P, Jat PS. Establishment of conditionally immortalized epithelial cell lines from both colon and small intestine of adult H-2Kb-tsA58 transgenic mice. Proceedings of the National Academy of Sciences of the United States of America 1993;90:587–591. [PubMed: 7678459]

Zhang Y, Forootan SS, Liu D, Barraclough R, Foster CS, Rudland PS, Ke Y. Increased expression of anterior gradient-2 is significantly associated with poor survival of prostate cancer patients. Prostate Cancer Prostatic Dis 2007;10:293–300. [PubMed: 17457305]

Zheng W, Rosenstiel P, Huse K, Sina C, Valentonyte R, Mah N, Zeitlmann L, Grosse J, Ruf N, Nurnberg P, Costello CM, Onnie C, Mathew C, Platzer M, Schreiber S, Hampe J. Evaluation of AGR2 and AGR3 as candidate genes for inflammatory bowel disease. Genes Immun 2006;7:11–18. [PubMed: 16222343]

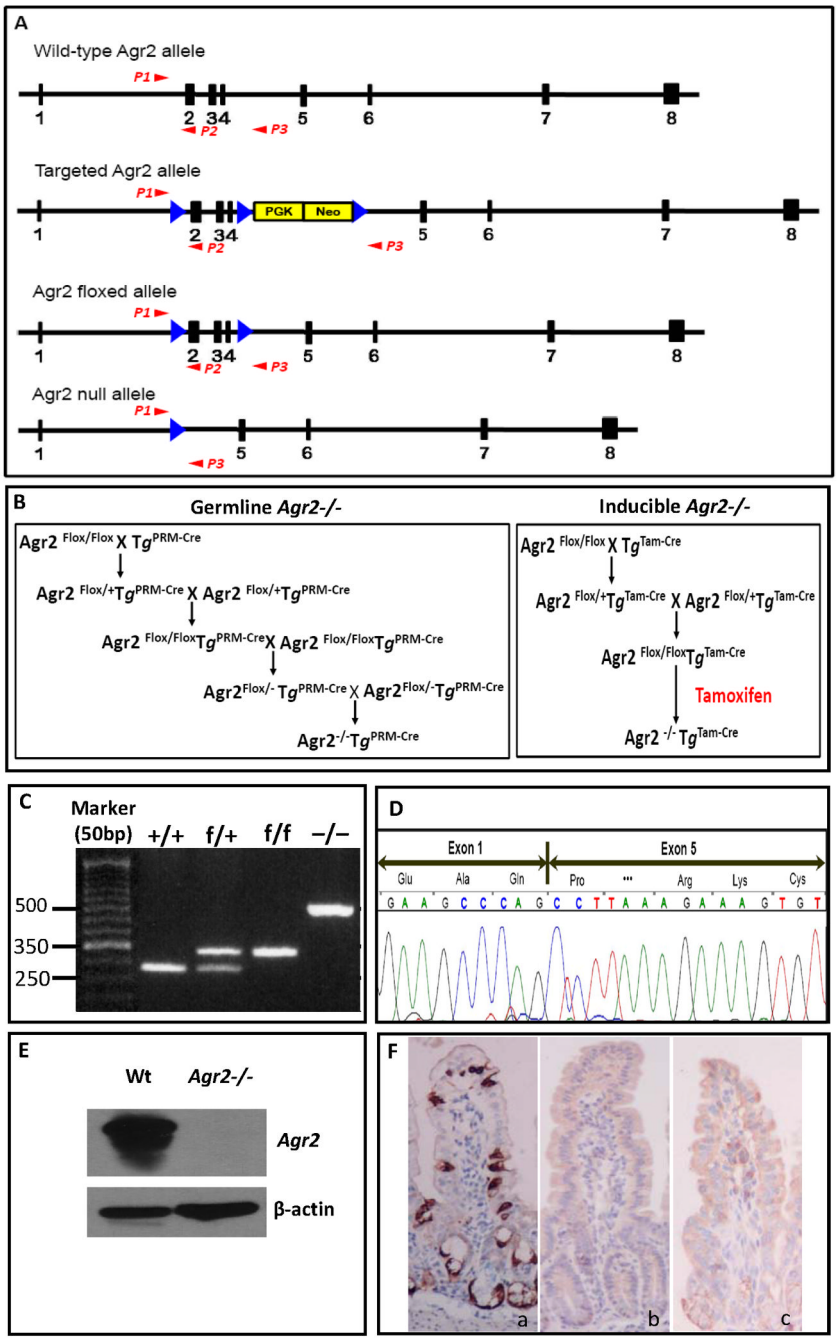

Figure 1.

Generation of *Agr2*−/− mice. (A) Gene-targeting strategy. The four alleles used in the gene targeting of *Agr2* are shown. Black boxes with numbers denote *Agr2* exons. PGK-Neo, neomycin resistance cassette, is shown as a yellow box. Blue arrows show LoxP sites. Red arrows P1–P3 depict PCR primer locations. Deletion of exon 2, 3 and 4 produces a frame shift in exon 5. (B) Breeding strategies for germline and inducible *Agr2* knockout mice. Flox, flanking LoxP site. *PRM-Cre*, protamine promoter driven *Cre* recombinase. *Tam-Cre*, tamoxifen inducible *Cre* recombinase. (C) PCR products from different *Agr2* genotypes. Mouse tail DNA was PCR amplified using three primers whose locations are shown in Panel A. The wild-type allele produced a band of 280bp, the floxed allele a band of 335bp and the

null allele a band of 519bp. (D) DNA sequencing of cDNA showing the junction of exons 1 and 5 in the *Agr2*−/− intestine epithelium. (E) Western analysis shows a 19.9-kDa band specific for *Agr2* absent in *Agr2*−/− mice. β-actin is used as a protein loading control. (F) Immunohistochemistry for *Agr2* in small intestine. *Agr2* protein is stained dark brown. (a) wild type; (b) germline *Agr2*−/−; (c) inducible *Agr2*−/−.

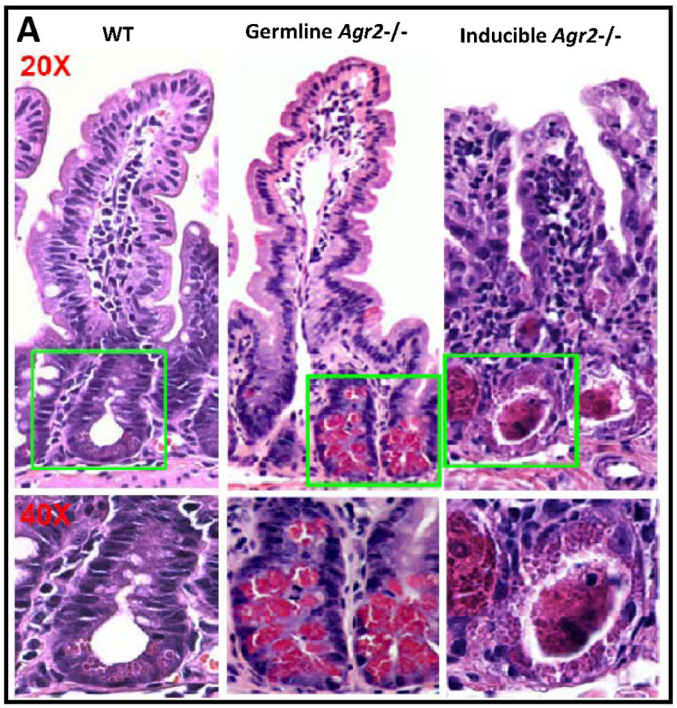

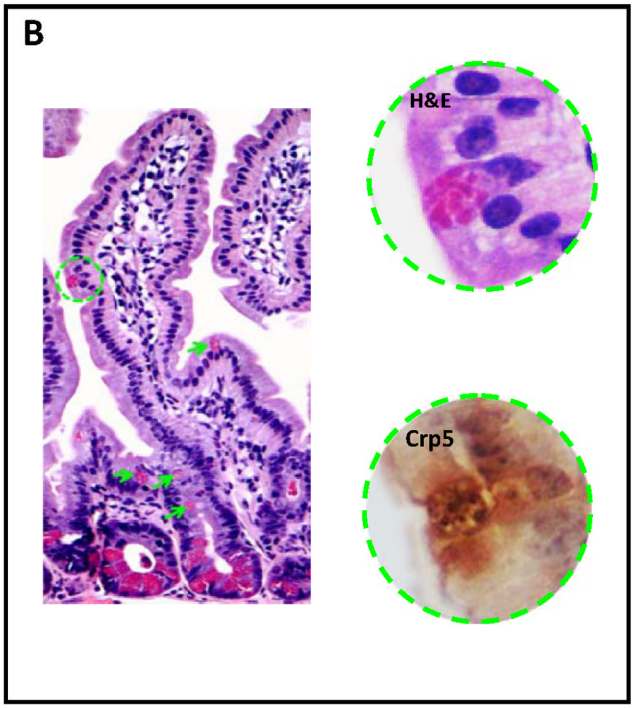

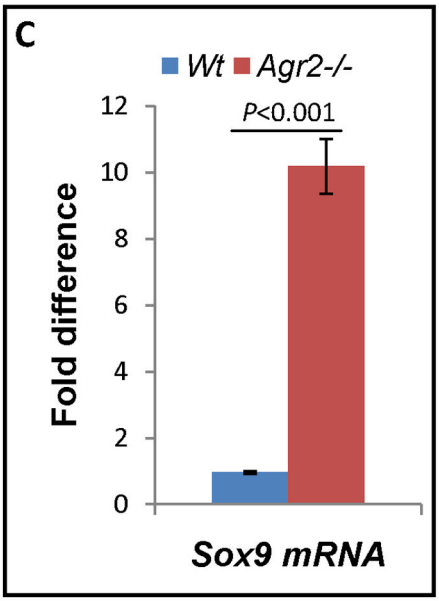

D

Mouse	P-60 fractions	Fraction #	Protein (μg)	Cryptdins (% of total protein in P-60 fractions)
Wt	Non-cryptdin	18-43	18307.4	
	Cryptdin	44-80	640.4	**3.4**
	Total		18947.8	
Agr2-/-	Non-cryptdin	18-43	23313.7	
	Cryptdin	44-80	2115.6	**9.1**
	Total		25429.4	

Figure 2.

Paneth cell abnormalities in germline and inducible *Agr2* −/− mice. (A) H+E stained sections of small intestine from wild type, germline and inducible *Agr2*−/− mice (day5). Paneth cells containing brightly eosinophilic granules are dramatically expanded in both germline and inducible *Agr2*−/− mice. Intralumenal Paneth cell granule casts are easily visible in the inducible *Agr2*−/− small intestine. Representative crypt bases are boxed in green and shown at 20× and 40× magnifications. A marked increase in lamina propria mononuclear infiltrates can also be seen in the inducible *Agr2*−/− small intestine. (B) Abnormally positioned Paneth cells in the upper crypt and villus epithelium of germline *Agr2*−/− mice. Multiple Paneth cells are ectopically located in the upper crypt (green arrows). A Paneth cell located on the villus is

indicated by a green circle. A 40× closeup image reveals characteristic Paneth cell granules that are cryptdin 5-positive by immunohistochemistry. (C) Increased Paneth cell marker Sox9 mRNA in inducible *Agr2*−/− small intestine (day6). TaqMan analysis of Sox9 mRNA in small intestine of inducible *Agr2*−/− and wild type mice. Wild-type Sox9 mRNA expression is normalized to 1.0. Mean bars of standard error are shown. The indicated P-values were determined by Student *t*-test. (D) Increased relative amount of cryptdins in the total protein extracted from distal small intestine of inducible *Agr2*−/− mice (day4). Bradford assays were performed to quantitate the amount of total protein in individual P-60 fractions from separations of inducible *Agr2*−/− and Wt P-60 fractions. Cryptdin P-60 fractions were those that appeared to contain mainly cryptdins by AU-PAGE. The total amount of protein was determined by adding the protein in non-cryptdin containing fractions to the protein in cryptdin containing fractions. Relative differences in the protein quantities between inducible *Agr2*−/− and Wt mice are listed.

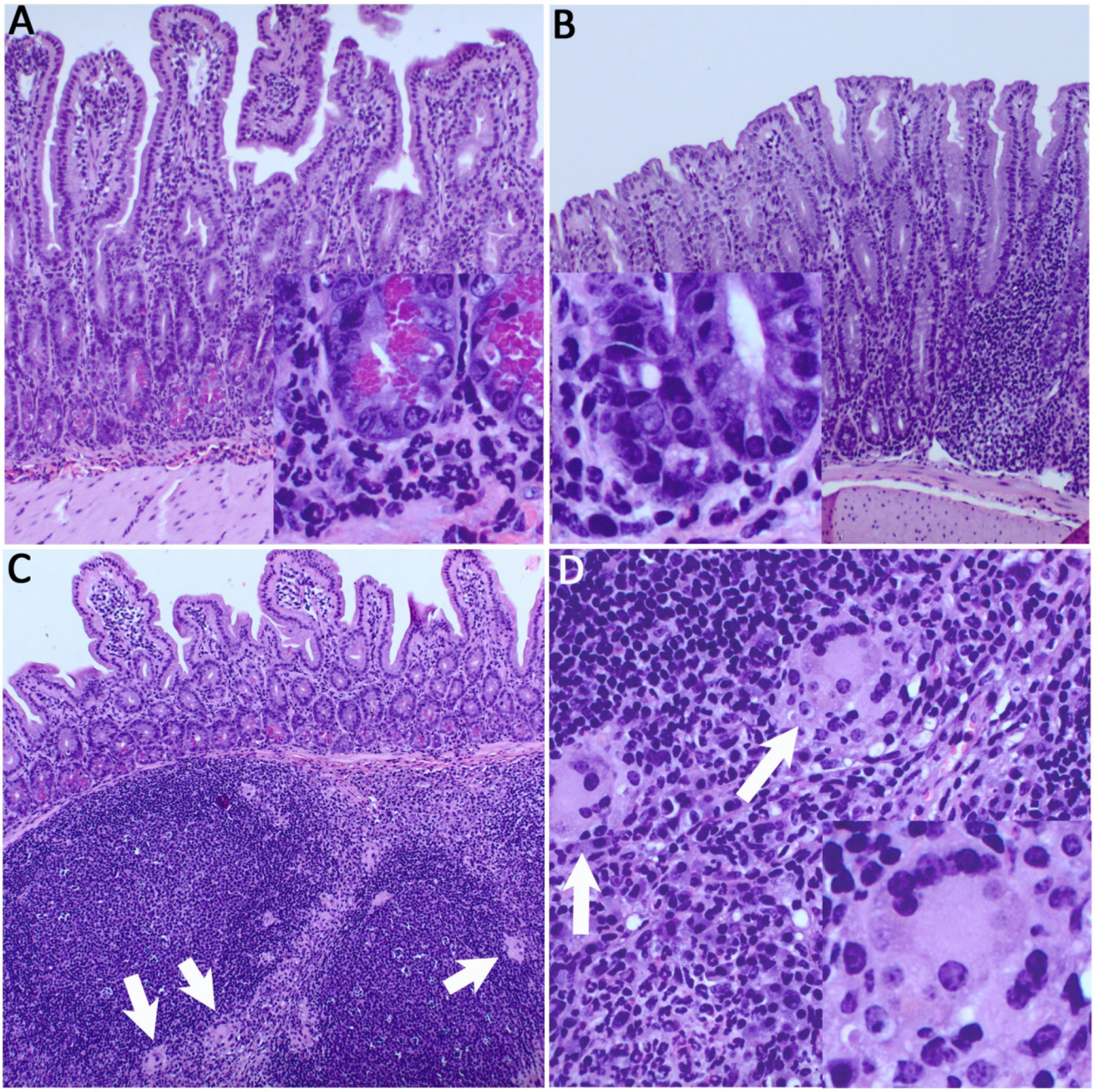

Figure 3.
Severe ileitis and colitis in germline *Agr2*−/− mice. (A) H&E staining reveals severe acute ileitis, with a dense, primarily neutrophilic infiltrate in the lamina propria and submucosa. Inset reveals neutrophils surrounding hypertrophied Paneth cells. (B) Acute colitis in the proximal colon, with loss of goblet cells, crypt elongation, and infiltrating neutrophils (inset). (C) Florid lymphoid hyperplasia of ileal Peyer's patches, with multinucleated giant cells (white arrows). (D) Multinucleated giant cells suggestive of granulomatous inflammation in interfollicular zones are seen at higher power (inset, lower right).

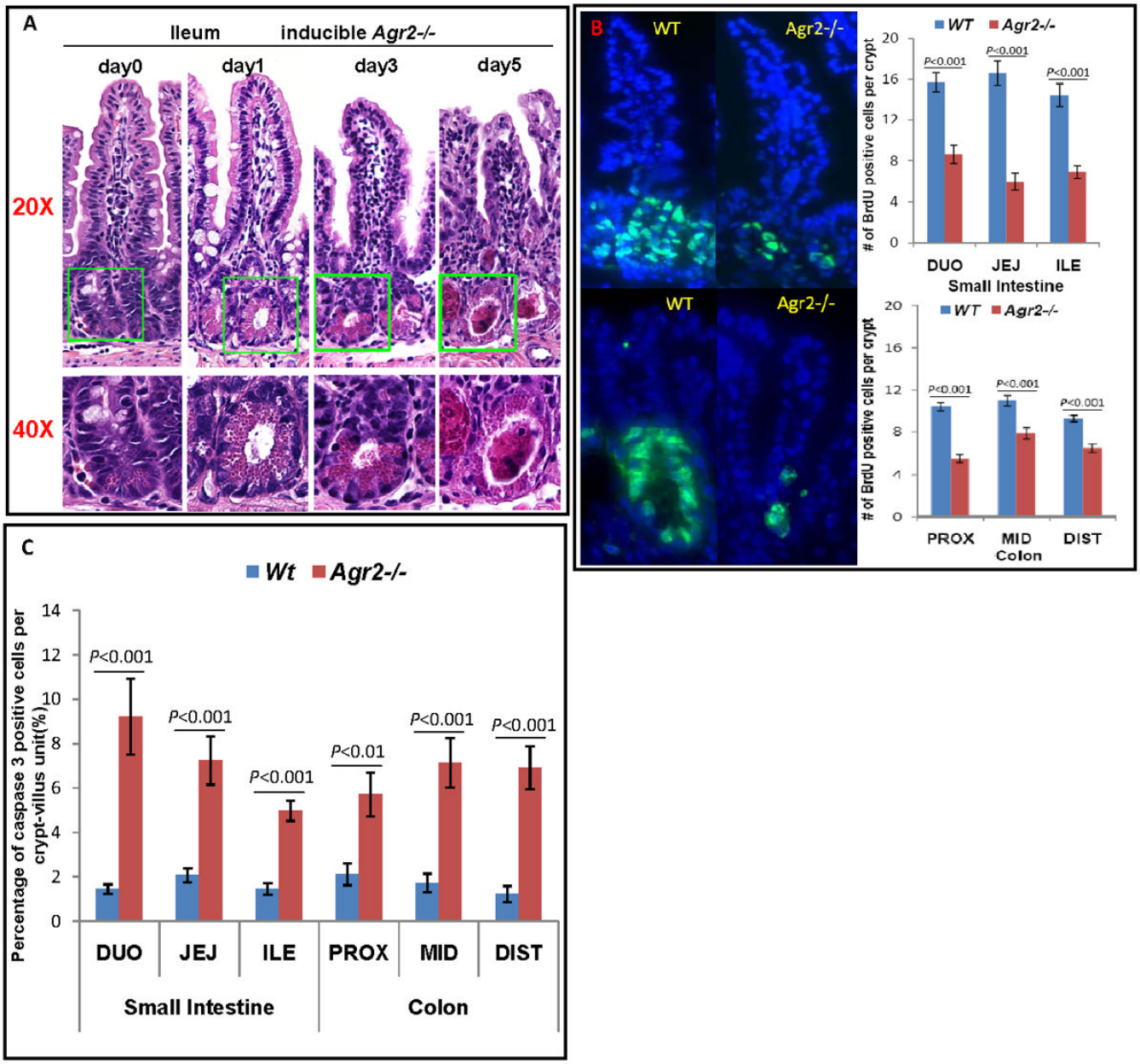

Figure 4.

Sequential abnormalities in morphology in the intestine of inducible *Agr2*−/− mice. (A) H&E staining shows sequential abnormalities of Paneth cells, goblet cells and enterocytes in inducible *Agr2*−/− small intestine. Representative crypt bases are boxed in green and shown at 20× and 40× magnifications. *Agr2* Tam-Cre flox/flox mice were injected with tamoxifen and mice analyzed over 1, 3 and 5 days. Day 0 (same day as tamoxifen injection), no visible abnormality. Day 1, crypt Paneth cell compartment expansion is seen, while goblet cells and enterocytes are unremarkable. Day 3, decrease in morphologically normal goblet cells, enterocyte dysplasia, further Paneth cell expansion and lamina propria inflammation is seen. Day 5, complete loss of morphologically normal goblet cells, severe loss of enterocytes, appearance of Paneth cell casts and increased lamina propria inflammation. (B) BrdU staining shows decreased proliferation in inducible *Agr2*−/− small intestine and colon (day6). Mice

were injected with BrdU and sacrificed 2 hours after injection. Small intestine (top) and colon (bottom) were visualized with fluorescence microscopy. (Left) Immunoflorescence of BrdU (green) labeled crypts from Wt and induced *Agr2*−/− mice. (Right) Number of BrdU positive cells per crypt in small intestine (top) and colon (bottom) of Wt mice and inducible *Agr2*−/− mice. (C) Caspase 3 assay shows increased apoptosis in inducible *Agr2*−/− small intestine and colon (day6). Mean bars of standard error are shown. The indicated P-values were determined by Student *t*-test.

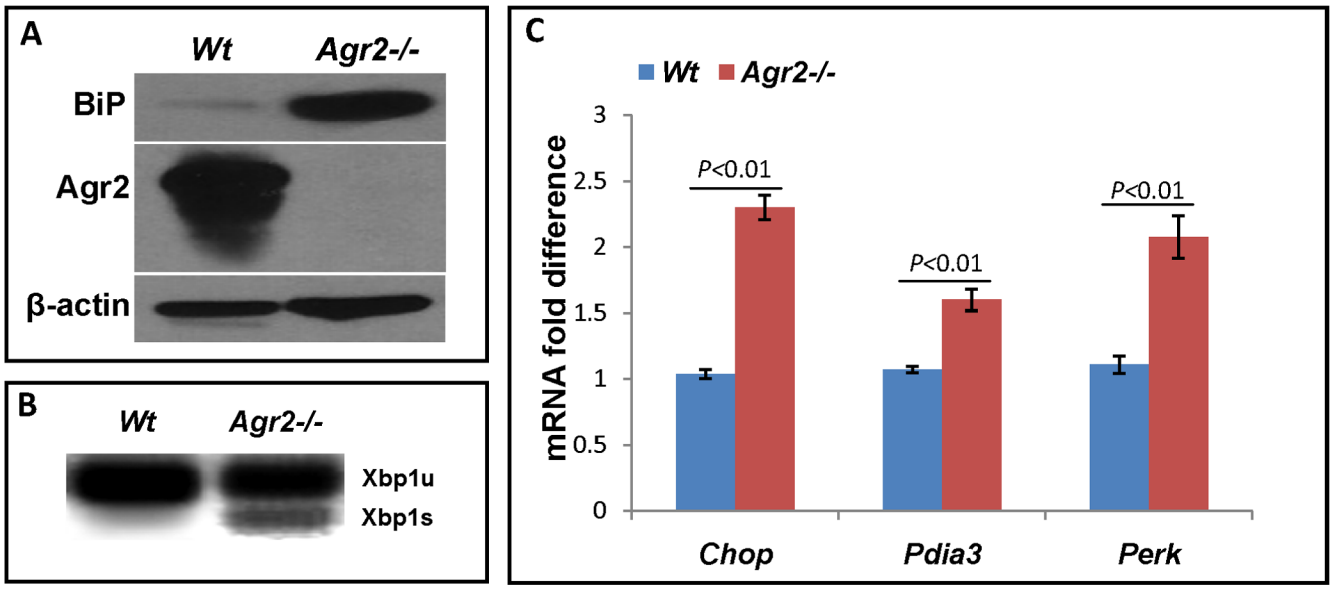

Figure 5.

Agr2 knockout increases ER stress in the intestine. (A) Germline *Agr2*−/− small intestine has increased levels of the ER stress response marker BiP. *Agr2* protein and actin loading control are shown below. (B) Inducible *Agr2*−/− small intestine (day6) has increased ER stress response marker Xbp1s. *Agr2* deletion was induced with tamoxifen and small intestine was assayed for Xbp1s mRNA on day6. Xbp1u, unspliced, full length form of Xbp1. Xbp1s, spliced form that is induced by ER stress. (C) Increased ER stress marker mRNA expression in induced *Agr2*−/− mice (day 6). qPCR of ER stress biomarker expression levels of Chop, Pdia3 and Perk. mRNA expressions of wild type are normalized to 1.0. Mean bars of standard error are shown. The indicated P-values were determined by Student *t*-test.

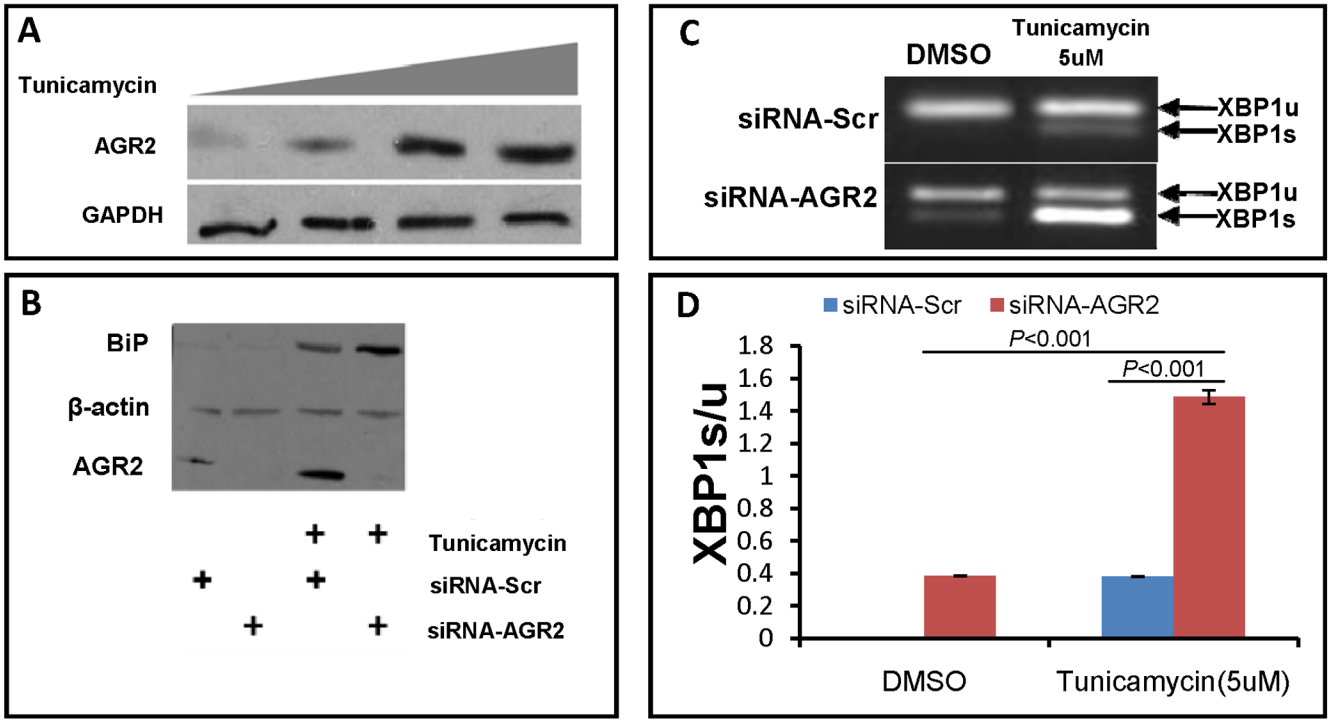

Figure 6.

AGR2 siRNA knock down increases ER stress. (A) *AGR2* is an ER stress response gene. Western blot analysis of SU86.86 cells in culture treated with increasing amounts of the ER stress inducer tunicamycin (0, 2.5, 5 and 7.5uM) and probed with anti-*AGR2* (Top) and anti-*GAPDH* as a loading control (bottom). (B) *AGR2* siRNA knockdown increases the ER stress biomarker *BiP* in tunicamycin treated cells. Western blot analysis of SU86.86 cells treated with 2.5uM tunicamycin and transfected with anti-*AGR2* siRNA. *BiP*, ER stress biomarker *BiP* (Top). Beta-actin is included as a loading control (Middle). *AGR2*, Anterior gradient 2 (bottom). *BiP*, beta-actin and *AGR2* all have different electrophoretic mobilities and were probed on the same transferred gel. SiRNA-Scr, negative control scrambled siRNA. SiRNA-*AGR2*, *AGR2* specific siRNA (Open biosystems). (C,D) RT-PCR of *XBP1* unspliced and spliced isoforms in SU 86.86 cells. *AGR2* siRNA knockdown induces *XBP1s* levels in SU 86.86 cells. Cells were treated with tunicamycin at 5uM, siRNA -*AGR2* increases *XBP1s* levels to much higher levels than siRNA-Scr, $P<0.001$. Standard error of the mean is shown. The indicated *P*-values were determined by Student *t*-test.